Quantum Black Holes Effects on the Shape of Extensive Air Showers

Nicusor Arsene,[1, 2, *] Lauretiu Ioan Caramete,[1, †] Peter B. Denton,[3, ‡] and Octavian Micu[1, §]

[1]*Institute of Space Science, P.O.Box MG-23, Ro 077125 Bucharest-Magurele, Romania*
[2]*Physics Department, University of Bucharest, Bucharest-Magurele, Romania*
[3]*Vanderbilt University, Nashville, TN 37235*
(Dated: October 9, 2013)

We investigate the possibility to find a characteristic TeV scale quantum black holes decay signature in the data recorded by cosmic rays experiments. TeV black holes can be produced via the collisions of ultra high energetic protons ($E > 10^{18} eV$) with nucleons the from atmosphere. We focus on the case when the black holes decay into two particles moving in the forward direction in the Earth reference frame (back-to-back in the center of mass reference frame) and induce two overlapping showers. When reconstructing both the energy and the shape of the resultant air shower, there is a significant difference between showers induced only via standard model interactions and showers produced via the back-to-back decay of black holes as intermediate states.

I. INTRODUCTION

Brane world models [1–3] or even four dimensional models with a large hidden sector of particles [4] have been suggested when trying to explain the large hierarchy between the strength of the gravitational force and the standard model. In this context quantum gravity can become important anywhere between the standard Planck scale (i.e. some 10^{16} TeV) and a few TeV. When the energy scale of gravity is in the lower end of this energy range (energies accessible for particle accelerators or in the center of mass of the collisions between ultra high energy cosmic rays and nucleons from the atmosphere) particle collisions can result in the creation of TeV mass black holes. This is a threshold effect in the sense that black hole creation turns on when the center of mass energy reaches the Planck scale.

Black holes formation via particle collisions has been studied since the 70's. The *Hoop conjecture* proposed by K. Thorne in 1972 [5] states that a black hole forms whenever the impact parameter b of two colliding objects (of negligible spatial extension) is shorter than the radius of the would-be-horizon (roughly, the Schwarzschild radius, if angular momentum can be neglected) corresponding to the total energy M of the system [6]

$$b \lesssim \frac{2\, l_{Pl}\, M}{M_{Pl}} \ . \tag{1}$$

This is intuitive but not enough to prove that black holes do indeed form in such collisions. However, there are now proofs (the first ones performed by Penrose who never published his findings) for the formation of closed trapped surfaces, which are enough to demonstrate gravitational collapse and hence black hole formation. Refs. [7–10] cover both the cases of zero and non-zero impact parameters. The analytical proof of Eardley and Giddings for the case of a four dimensional space-time [10] demonstrates the formation of classical black holes due to the collisions of two particles with a non-zero impact parameter at energies much larger than the Planck mass. The proof was extended to the semi-classical regime (semi-classical black holes are objects with masses in the range from 5 to 20 times the Planck mass [11]) by Hsu [12].

Many articles have considered semi-classical TeV mass black holes production at particle colliders or in the cosmic ray data [13–21]. The possibility also exists for the energy in the center of mass not to be large enough for semi-classical black holes to be produced and it was proposed [22–24] to also consider quantum black holes. These are non-thermal objects with masses up to five Planck masses which are also easier to produce. Because they are non-thermal, quantum black holes are expected to decay into a small number of particles, typically two. Experimental signatures for such decays are very different from the one of semi-classical objects which are expected to decay into several particles in a final explosion, see e.g. [25, 26] for recent reviews.

Refs. [27, 28] investigate the possibility to detect the back-to-back decays of TeV scale quantum black holes by observing double shower events (showers having common origins and developing at an angle) in the cosmic ray data or similar events in the data recorded by neutrino observatories. In the latter case one would observe muon tracks starting from a common origin and oriented at an angle. Such black holes are produced in the collisions between protons or neutrinos with energies above 10^{17} eV and nucleons from the atmosphere respectively water or ice. The black holes immediately decay into two standard model particles. The decays for which two distinct showers are visible represent less than one percent from the total number of black hole events. Ref. [29] discusses experiments and simulations of the presence of multi-core showers. In 99.9% of the cases the two showers overlap entirely.

It needs to be pointed out that this signature, along with the ones proposed in Refs. [27, 28] are complemen-

tary to the TeV scale gravity searches performed by the various experimental groups from the Large Hadron Collider (LHC) [30, 31]. As it will become obvious later, the signature proposed here actually allows the community to look for the scale of gravity in the tens of TeV regime, energies beyond the reach of any current particle physics experiment.

In this article we study the possibility to distinguish the extensive air showers induced by back-to-back black hole decays from standard showers. Experiments such as Pierre Auger Observatory [32] and Telescope Array [33] can evaluate the shape of showers with their fluorescence detectors and the energy deposited by the shower in surface detectors. The proposed space based JEM-EUSO experiment [34] will provide an additional means to detect the shape of showers at energies above 10^{19} eV. The fluorescence detectors are used to determine the mass composition of primary particle by measuring the atmospheric depth where the density of charged particles is maximum (so called X_{max}) and at the same time to estimate the energy of the primary particle by integrating the Gaisser-Hillas curve [35] and multiplying by a mean energy loss rate in the atmosphere of 2.19 MeV/g cm^{-2}. For the Pierre Auger Observatory, the energy of the primary particle can also be calculated using the energy deposited in the grid of surface detectors which consists in 1600 water Cherenkov tanks placed at a distance of 1.5 km each other, and are dedicated to measure the lateral distribution function (LDF) of the showers. Using the signal recorded by detectors situated 1000 meters away from the shower axis, S(1000), one can estimate the energy of primary particle.

The findings of the present article are based on a set of extensive air shower simulations made using CORSIKA 6.990 (COsmic Ray SImulations for KAscade) [36, 37] for micro black holes produced by protons with energies of 10^{18} eV which interact with nuclei in the atmosphere. The black holes decay immediately back-to-back into two particles, in our case a pair of pions (their electric charges do not have any significant effect on the resulting showers), which have approximately equal energies in the center of the laboratory reference frame. The two black hole decay products then produce overlapping extensive atmospheric showers.

II. BLACK HOLES PRODUCTION

The number of black holes expected to be produced within the volume of the atmosphere visible to a cosmic rays experiment, taking into account the experiment's dimensions and the duty cycle of the detectors, is given by

$$N = \int dE N_A \frac{d\Phi}{dE} \sigma(E) A(E) T \qquad (2)$$

where $\sigma(E)$ is the production cross section described bellow, $\frac{d\Phi}{dE}$ is the flux of cosmic ray particles, $A(E)$ is the

acceptance of the experiment measured in cm^2 sr yr, N_A is Avogadro's number and T is the running time of the detectors.

The cross section p N $\rightarrow$ BH is given by:

$$\sigma^{pN}(s, x_{min}, n, M_D) = \int_0^1 2z dz \int_{\frac{(x_{min} M_D)^2}{y(z)^2 s}}^1 du \qquad (3)$$
$$\times \int_u^1 \frac{dv}{v} F(n) \pi r_s^2(us, n, M_D)$$
$$\times \sum_{i,j} f_i(v, Q) f_j^N(u/v, Q)$$

where M_D is the $4+n$ dimensional reduced Planck mass, $z = b/b_{max}$, $x_{min} = M_{BH,min}/M_D$, n is the number of extra-dimensions, $F(n)$ and $y(z)$ are the factors introduced by Eardley and Giddings [10] and by Yoshino and Nambu [38]. The $4+n$ dimensional Schwarzschild radius is given by

$$r_s(us, n, M_D) = k(n) M_D^{-1} [\sqrt{us}/M_D]^{1/(1+n)} \qquad (4)$$

where

$$k(n) = \left[2^n \sqrt{\pi}^{n-3} \frac{\Gamma((3+n)/2)}{2+n} \right]^{1/(1+n)}. \qquad (5)$$

The number of the black holes depends directly on the flux of the cosmic ray particles. It is important to note that the composition of the cosmic ray flux includes neutrons, protons, light and intermediate nuclei, heavier nuclei like Fe [39], but also neutrinos. Since the protons are the main constituent particles in the cosmic ray flux at 10^{18} eV, we select protons as primary particles to perform our analysis and comparisons.

III. BLACK HOLES DECAY

We wish to analyze the signature generated by the two overlapping showers induced by the decay products of a quantum black hole. This is an extension of the cases studied previously in [27, 28]. More specifically, in the previous papers the authors analyzed the possibility for the particles resulting from the back-to-back decay of quantum black holes to generate showers which are separated spatially. As it turned out, only for less than 1% of the quantum black hole decays are the two showers separated spatially. In this article we analyze the signature of the events in which quantum black holes decay into a pair of pions (which could be any of the π^0, π^+, π^- depending on the intermediary quantum black hole charge), particles which then induce two overlapping showers. Numerical simulations show that at these energies, the showers look exactly the same regardless of the charges of the two initial pions. Because of the heavy simulations involved we focus on one case only, more specifically the case in which the two pions have roughly equal energies in the Earth reference frame.
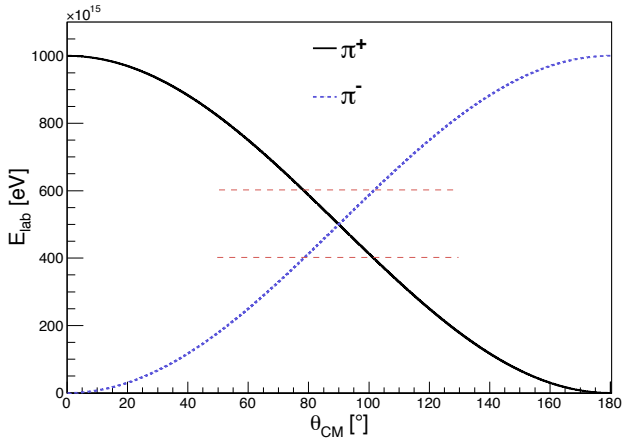
FIG. 1. The energies of the two resulting particles (for our simulations we consider a π^+ and π^-) in the Earth reference frame a a function of the decay angles measured from the direction of propagation of the quantum black hole in the center of mass frame. The red dotted lines highlight the intervals of angles for which the energies of the two particles vary between $4 \times 10^{17} - 6 \times 10^{17}$ eV.

The process of black hole formation requires for the impact parameter b (defined as the perpendicular distance between the paths of the two particles that are colliding) to be smaller than the horizon radius and we will only consider the events for which this inequality holds. Also in the process of black hole formation via particle collisions, some energy is radiated as gravitational radiation. We will work with a further simplifying assumption, which is that the whole energy of the two particles, including the partons of the protons goes into the black hole creation. Using a simple relativistic textbook calculation [27, 28] one can calculate the black hole mass M_{BH} and relativistic Lorentz factor γ_{BH}.

As stated before, quantum black holes are non-thermal objects which decay into a small number of particles, most likely into two particles moving back-to-back in the center of mass reference frame and with no preferred direction with respect to the direction of motion of the black hole. The main constraints on the decay are for the sum of the masses of the two resulting particles to be smaller than the black hole mass M_{BH} and for standard model charges to be conserved.

Under the assumptions stated above, when a proton having an energy of 10^{18} eV collides with a nucleon in the atmosphere, the resulting quantum black hole mass is on the order of $M_{BH} \simeq 4 \times 10^{13}$ eV and the black hole is moving relativistically with gamma factor of $\gamma_{BH} \simeq 2 \times 10^4$. Such large gamma factors have significant impact on the angle between the trajectories of the two particles when viewed from the Earth reference frame. Also the energies of the two particles, when measured in this reference frame, vary due to a combination of the Lorentz factor of the center of mass and the directions at which the two particles move in the center

of mass reference frame with respect to the direction of motion of the center of mass. These dependencies are encoded in the Lorentz transformation formulas and for the particular case discussed here this dependency is shown in Fig. 1. The plot represents the energy in the laboratory/Earth reference frame as a function of the angle that the trajectories of the particles make in the center of mass measured with respect to the direction of motion of the center of mass. Because of limited computational power (one simulation requires one processor core to run at full power on the order of a week) we limit our simulations to the case in which the energies of the two particles (in the Earth reference frame) are roughly equal. Therefore the present analysis will apply to those cases. One might extend the simulations for energies which vary on a broader range (one with respect to the other). Therefore, for our case of interest we select the interval of angles for which the two pions have energies between $4 \times 10^{17} - 6 \times 10^{17}$ eV. This happens for $75° \leq \theta_{CM} \leq 105°$. One can easily calculate that for 25.8% of the total number of quantum black holes produced the particles resulting from their back-to-back decay are emitted in this interval of angles.

Using this range of angles, together with the acceptance for the Pierre Auger Observatory [40] and a fit for the cosmic ray flux [41] in Eq. 2 one can estimate the number of events of this type that are expected to be seen in the Pierre Auger Observatory data. Another ingredient needed in Eq. 2 is the extra-dimensional scenario considered and we will analyze the cases for $n = 0, 1, 4, 5, 6, 7$ extra dimensions, where the case $n = 0$ refers to a scenario with no extra-dimensions but in which low scale gravity is due to the existence of a large hidden sector of particles which interact only gravitationally [4]. Also the case $n = 1$ corresponds to the Randall-Sundrum model since the ADD scenario with one extra-dimension is already excluded by other experiments.

The number of quantum black holes which can be created also depends on the value of the Planck scale. As stated before we are interested in quantum black holes which have masses between one and five Planck masses. Considering that a 10^{18} eV cosmic ray produces a black hole on the order of 40 TeV, this is a quantum black hole only if the Planck scale is around 5 TeV or greater. This means that this signature can be used to search for the possibility that the Planck scale is above 5 TeV and so a natural extension of the LHC searches. Table I shows the number of quantum black holes for which the energies of the two particles they decay into are between $4 \times 10^{17} - 6 \times 10^{17}$ eV when measured in the Earth reference frame as function of the number of extra-dimensions and the value of the Planck mass.

One more question needs to be addressed, which is: how can one differentiate this signature from the QCD background since also QCD events can result in two high energetic jets via processes of the type $q + \bar{q} \rightarrow$ dijets and $q + g \rightarrow$ dijets. What one needs to have in mind is that the number of QCD events of this type is strongly suppressed by a factor α_S^2 (where α_S is the QCD coupling constant

No. of extra dimensions	$M_{Pl} = 5$ TeV	$M_{Pl} = 6$ TeV	$M_{Pl} = 7$ TeV	$M_{Pl} = 8$ TeV	$M_{Pl} = 9$ TeV	$M_{Pl} = 10$ TeV
0	28.94	13.96	7.53	4.42	2.76	1.81
1	196.27	113.58	71.53	47.92	33.65	24.53
4	1173.41	757.56	523.29	379.81	286.28	222.32
5	1569.25	1025.50	715.69	524.10	398.16	311.38
6	1983.28	1307.37	919.13	677.37	517.49	406.74
7	2411.03	1599.72	1130.87	837.40	642.45	506.86

TABLE I. Number of black hole events per year expected at the Pierre Auger Observatory experiment for which the angle between the direction of the two decaying particles and the direction of motion of the quantum black hole lies in the interval between $75° - 105°$ in the center of mass frame.

squared divided by 4π) compared to the gravitationally induced events. At the scale $M_P \sim$ TeV, $\alpha_S^2 \sim 8 \times 10^{-3}$, we thus expect about 100 times more events of this type above the QCD background if the Planck mass is in the TeV region, while for a larger Planck mass the QCD background is even smaller due to asymptotic freedom.

IV. SIMULATIONS AND RESULTS

CORSIKA is a code based on Monte Carlo methods, dedicated to simulate in detail the development of extensive air showers in the atmosphere. For our simulations we chose the altitude, observation plane and magnetic field for the position of the Pierre Auger Observatory. CORSIKA also allows performing cuts for the energies of the particles. For the simulations performed energy cuts of the secondary particles are set at 300 MeV for hadrons and for muons; and 3 MeV for electromagnetic component. For the simulations we use the QGSJET 01C model [42] for high energy hadronic interactions.

Further, we wish to analyze if there is a distinctive signature for an extensive air shower produced via the back-to-back decay into two particles of a black hole when compared with a standard air shower produced by protons. In each of the cases the starting particles are protons with energies of 10^{18} eV. For what we call standard air showers the protons interact with nuclei from the atmosphere and produce the usual showers which are recorded by cosmic ray observatories. We call "black hole induced showers" the showers for which protons first interact with nucleons to create quantum black holes. The black holes decay instantaneously back to back into two particles (for our simulations we consider that the two black hole decay products are a π^+ and a π^-) which are highly boosted forward in the Earth reference frame. We perform numerical simulations for the case when the two pions have roughly equal energies on the order of 5×10^{17} eV. Of course these pions further interact with nucleons to produce extensive air showers. In the following paragraphs we make a thorough comparison between standard proton induced showers and black hole induced showers. For this purpose, the primary interaction point is taken at 20 km altitude in both types of simulations. This is the average altitude at which protons with this energy moving vertically first interact in the atmosphere.

Fig. 2 shows a comparison between the X_{max} value for these two cases. A shift of approximately 40 g/cm² is observed for the case of a black hole induced shower when compared with a standard model shower. One can see that the X_{max} value for black hole induced showers is the lowest one. Note that this difference is significant, considering that the difference in X_{max} between a proton shower and iron nucleus shower at the same energy is $X_{max}^p - X_{max}^{Fe} \simeq 100$ g/cm². This difference can be observed by the fluorescence detectors of the cosmic ray observatories.

The second observable which is estimated when the cosmic ray observatories analyze their data is the energy of the primary particle using the energy released in the ground detectors (for experiments where they are available). The Pierre Auger Collaboration estimate the energy of the primary particle by using the signal recorded by the ground detectors situated 1000 meters away (S(1000)) from the shower axis [32]:

$$E(EeV) = 0.12\left(\sqrt{1 + 11.8(sec\,\theta - 1)^2}\,S(1000)\right)^{1.05} \quad (6)$$

where θ represents the zenith angle of the incoming primary particle.

The signal in the ground detectors is directly proportional with the density of charged particles and with the momentum carried by the charged particles and the energy of the primary particle depends on these values as it was seen in Eq. 6.

Fig. 3 represents the lateral distribution function of charged particles at the observation level (as a reminder this part of the analysis is pertinent to cosmic ray observatories which can record the particles which arrive on the ground) and their global momentum, both as functions of the distance from the shower axis. We observe that both the density of charged particles and their momenta are greater for the case of standard model showers
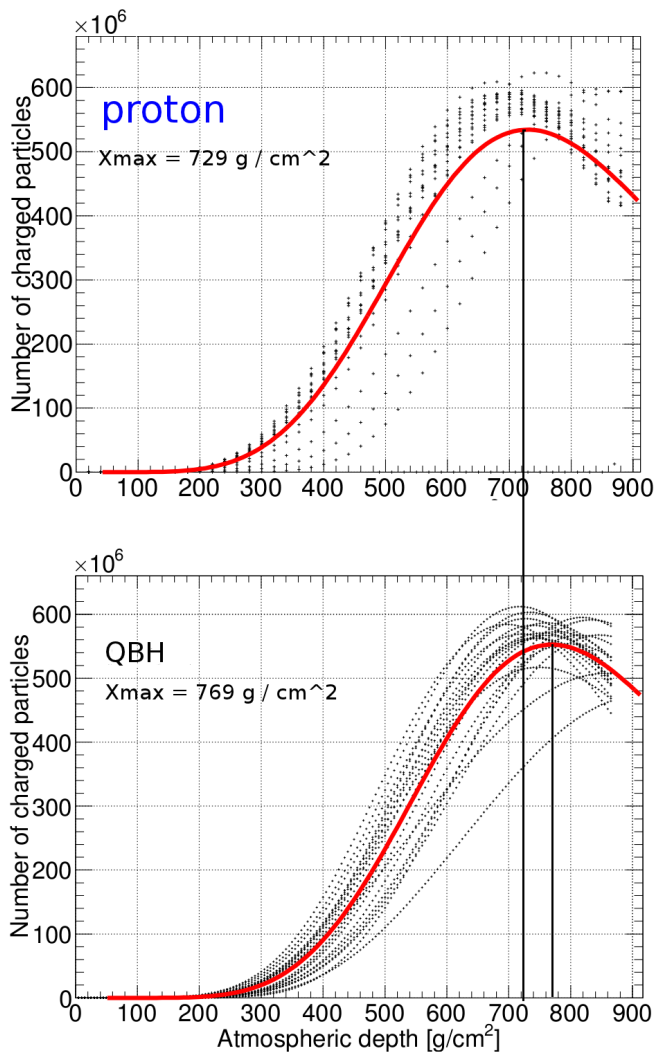
FIG. 2. Longitudinal profiles of extensive air showers simulated with CORSIKA. Each of the plots contain 20 simulations. The plot on top shows standard model induced showers of energies $E = 10^{18}$ eV. The lower plot contains twenty black hole induced shower simulations. In this case the primary particles were $E = 10^{18}$ eV protons which produced quantum black holes that decayed into two pions with roughly equal energies in the laboratory reference frame. Black dots represent the number of charged particles for each simulation and the red lines represent the fits with Gaisser-Hillas function to obtain the mean values of X_{max}. The vertical black lines are used to emphasize the shift in X_{max}.

in comparison with black hole induced showers.

While the integrals of the curves in Fig. 3 should be equal, they aren't due to saturation of the detectors in the core of the shower where the quantum black hole case dominates the standard model case.

Fig. 4 represents a zoom in of Fig. 3 in the region from 950 to 1050 meters from the shower axis. The ratio of the number of charged particles for the two types of events is:

$$\frac{\rho_{ch}^p}{\rho_{ch}^{qBH}} \simeq 1.25, \tag{7}$$

with ρ_{ch}^p representing the number of charged particles for a standard proton shower and ρ_{ch}^{qBH} the number of charged particle for the case of a black hole decay induced event.

One can also estimate the ratio of the global momentum for a standard model shower p_{ch}^p to the one for a black hole type of event p_{ch}^{qBH}

$$\frac{p_{ch}^p}{p_{ch}^{qBH}} \simeq 1.33. \tag{8}$$

Remembering that for all simulations the initial energies were the same, these plots show that the surface detectors will underestimate the energy of the primary particle by 25-30% when the showers are generated with intermediary quantum black hole states.

Putting everything together one realizes that if quantum black holes are created as intermediary states the extensive air showers look very different from typical proton generated showers. The atmospheric depth for which the density of charged particles is maximum increases, while the energy calculated from the number of charged particles which reach the ground and their momenta is underestimated by 25-30%. Fig. 5 shows the variation of X_{max} as a function of the energy. The plot presents the Pierre Auger data compared to air shower simulations for several hadronic models. It also includes the data point representing the results of the simulations for extensive air showers produced via back-to-back black hole decays.

Recapitulating shortly, for our simulations we considered 10^{18} eV protons which produced quantum black holes by interacting with nucleons in the atmosphere. The quantum black holes decayed back-to-back into a pair of pions. In 25.8% of the cases the energies of the pions are approximately equal in the reference frame of the experiment with values on the order of 5×10^{17} eV. The

two pions produce overlapping showers. The simulations show for these two overlapping showers an $X_{max} = 769$ g/cm^2 (40 g/cm^2 larger than for protons when using the same interaction model). When estimating the energy of the primary cosmic ray using the energy deposited in the ground detectors one finds it to be 7.7×10^{17} eV. This energy needs to be compared with the 10^{18} eV benchmark
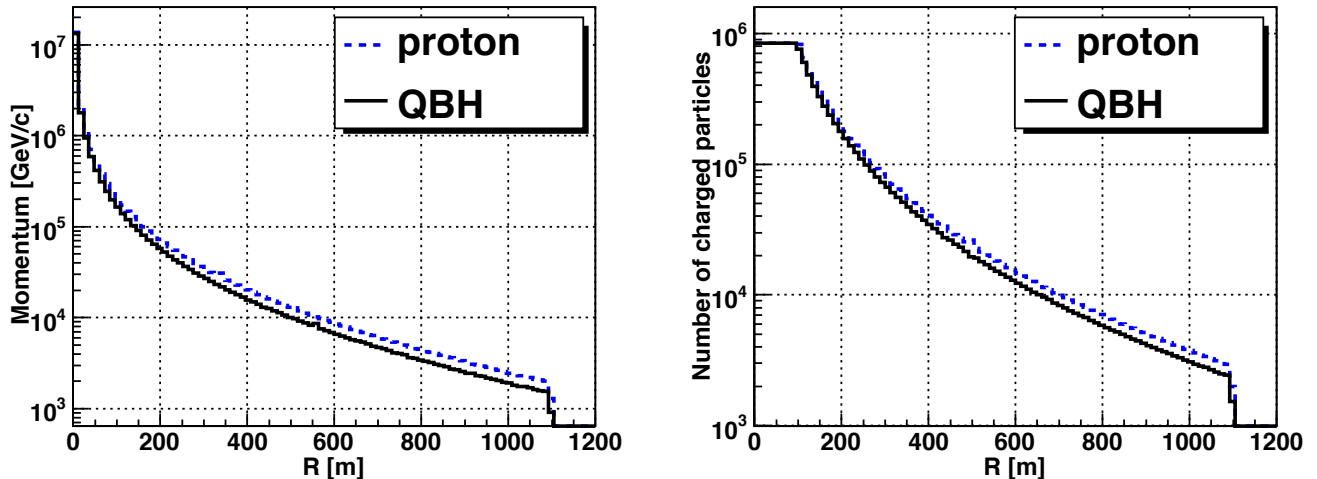
FIG. 3. The total momentum carried by the charged particles at observation level versus the distance from shower axis (left), respectively number of charged particles versus the distance from shower axis (right). The blue dashed line represents the benchmark case (standard proton showers), while the continuous black line represents the black hole induced showers. These are the average values calculated over the same twenty simulations from Fig. 2.
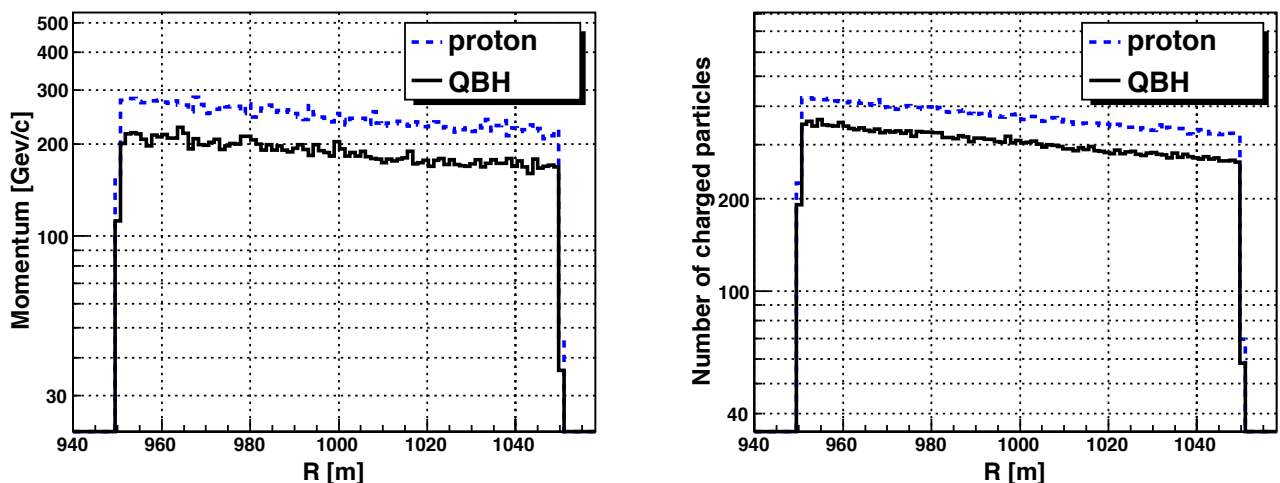

FIG. 4. The total momentum carried by the charged particles at roughly 1000 meters from the shower axis versus the distance from shower axis (left), respectively number of charged particles at roughly 1000 meters from the shower axis versus the distance from shower axis (right). The blue dashed line represents the benchmark case (standard proton showers), while the continuous black line represents the black hole induced showers. These are the average values calculated over the same twenty simulations from Fig. 2.

energy, which is the energy one estimates for the protons by performing the same analysis. The systematic errors when estimating the energy are around 22%. The standard deviations of the X_{max} value are ± 40 g/cm^2 for the quantum black hole induced showers and ± 35 g/cm^2 for the standard model showers. The error bars are represented on the final plot. Only simulations for the primary particles having energies of 10^{18} eV were performed because of the lack or more computer power. A simulation of this type takes on the order of a week and the time

scale increases with the energy of the primary particle due to the much larger number of particles produced in the showers. Given the steady increase of X_{max} with the energy in the numerical simulations shown in Fig. 5 we have strong reason to believe that the same behavior will be present when performing numerical simulations for quantum black hole induced showers. Even so, we will not rely on this assumption but perform simulations at higher energies, but this will be a lengthy process and

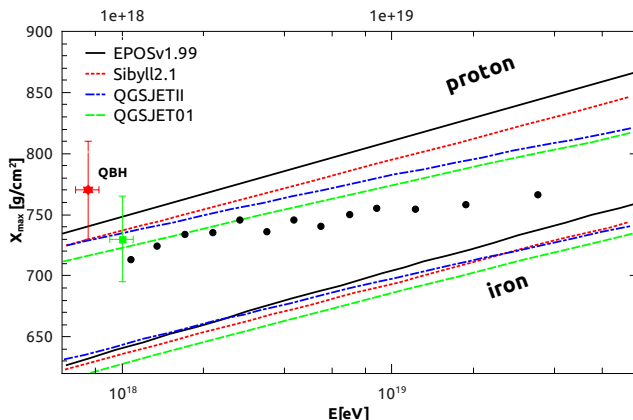the findings will be presented in a subsequent letter.

FIG. 5. Variation of the atmospheric depth for which the density of charged particles is maximum - X_{max} as a function of the energy. The plot presents the Pierre Auger data compared to air shower simulations [43] for different hadronic models [44–47]. In addition we include the case of black holes induced events for the simulations presented above. The energies of the primary particles used as input in our simulations were 10^{18} eV. The error bars for our data point represent the RMS of X_{max}. The red dot represents the case in which there is an intermediary quantum black hole, while the green dot represents our numerical simulations for the standard proton induced showers. The simulations were performed using the QGSJET01 model.

V. CONCLUSIONS AND OVERLOOK

While present day particle accelerators allow us to test for the Planck scale up to the 10 TeV region, ultra high energy cosmic ray observatories provide a unique opportunity to go one order of magnitude higher in energy. At the same time, complementary searches to the ones done at the LHC can be performed. The Planck scale can be searched for via non-thermal quantum black hole decay signatures. Above the quantum gravity scale quantum black holes can be created via the collisions of ultrahigh energy cosmic rays with nucleons from the atmosphere. These holes decay instantaneously preferentially into two particles which produce two overlapping hadronic showers.

The resulting showers have different profiles and X_{max} values when compared with similar showers generated via purely standard model processes (without intermediary quantum black hole states). The shift in X_{max} is of approximately 40 g/cm^2 for the case of a 10^{18} eV primary ultrahigh energy proton. On top of this, the primary particle energies estimated using the momentum carried by charged particles recorded by detectors situated at roughly 1000 meters from the shower axis are underestimated by 25-30% in the cases when intermediary quantum black hole states are present, as it was shown previously.

Therefore, we conclude that this signature is a very suitable one to be used for performing quantum black hole searches in the data recorded by cosmic ray observatories. When discovered above a certain energy, this signature would be a clear indication of the presence of a threshold such as the one due to getting above the value of the Planck scale. Due to limited computer power only simulations at 10^{18} eV oriented vertically towards the Earth and with the primary interaction point at an altitude of 20 km were performed so far. It is in our future plan to perform more numerical simulations over a broader range of energies, oriented at different angles with respect to the ground and having the primary interaction points at random altitudes.

[1] N. Arkani-Hamed, S. Dimopoulos, and G. Dvali, Phys.Lett. **B429**, 263 (1998), arXiv:hep-ph/9803315 [hep-ph].

[2] I. Antoniadis, N. Arkani-Hamed, S. Dimopoulos, and G. Dvali, Phys.Lett. **B436**, 257 (1998), arXiv:hep-ph/9804398 [hep-ph].

[3] L. Randall and R. Sundrum, Phys.Rev.Lett. **83**, 3370 (1999), arXiv:hep-ph/9905221 [hep-ph].

[4] X. Calmet, S. D. Hsu, and D. Reeb, Phys.Rev. **D77**, 125015 (2008), arXiv:0803.1836 [hep-th].

[5] K. S. Thorne, "Nonspherical Gravitational Collapse–A Short Review," in *Magic Without Magic: John Archibald Wheeler*, edited by J. R. Klauder (1972) p. 231.

[6] We shall use units with $c = \hbar = 1$ and the Boltzmann constant $k_B = 1$, and always display the Newton constant $G = l_{Pl}/M_{Pl}$, where l_{Pl} and M_{Pl} are the Planck length and mass, respectively.

[7] P. D'Eath and P. Payne, Phys.Rev. **D46**, 658 (1992).

[8] P. D'Eath and P. Payne, Phys.Rev. **D46**, 675 (1992).

[9] P. D'Eath and P. Payne, Phys.Rev. **D46**, 694 (1992).

[10] D. M. Eardley and S. B. Giddings, Phys.Rev. **D66**, 044011 (2002), arXiv:gr-qc/0201034 [gr-qc].

[11] P. Meade and L. Randall, JHEP **0805**, 003 (2008), arXiv:0708.3017 [hep-ph].

[12] S. D. Hsu, Phys.Lett. **B555**, 92 (2003), arXiv:hep-ph/0203154 [hep-ph].

[13] S. Dimopoulos and G. L. Landsberg, Phys.Rev.Lett. **87**, 161602 (2001), arXiv:hep-ph/0106295 [hep-ph].

[14] T. Banks and W. Fischler, (1999), arXiv:hep-th/9906038 [hep-th].

[15] S. B. Giddings and S. D. Thomas, Phys.Rev. **D65**, 056010 (2002), arXiv:hep-ph/0106219 [hep-ph].

[16] J. L. Feng and A. D. Shapere, Phys.Rev.Lett. **88**, 021303 (2002), arXiv:hep-ph/0109106 [hep-ph].

[17] L. A. Anchordoqui, J. L. Feng, H. Goldberg, and A. D. Shapere, Phys.Lett. **B594**, 363 (2004), arXiv:hep-ph/0311365 [hep-ph].

[18] L. A. Anchordoqui, J. L. Feng, H. Goldberg, and A. D. Shapere, Phys.Rev. **D65**, 124027 (2002), arXiv:hep-ph/0112247 [hep-ph].

[19] L. A. Anchordoqui, J. L. Feng, H. Goldberg, and A. D. Shapere, Phys.Rev. **D68**, 104025 (2003), arXiv:hep-ph/0307228 [hep-ph].

[20] M. Kowalski, A. Ringwald, and H. Tu, Phys.Lett. **B529**, 1 (2002), arXiv:hep-ph/0201139 [hep-ph].

[21] A. Ringwald and H. Tu, Phys.Lett. **B525**, 135 (2002), arXiv:hep-ph/0111042 [hep-ph].

[22] X. Calmet, W. Gong, and S. D. Hsu, Phys.Lett. **B668**, 20 (2008), arXiv:0806.4605 [hep-ph].

[23] X. Calmet, D. Fragkakis, and N. Gausmann, Eur.Phys.J. **C71**, 1781 (2011), arXiv:1105.1779 [hep-ph].

[24] X. Calmet, D. Fragkakis, and N. Gausmann, Chap. 8 in A.J. Bauer and D.G.Eiffel editors,Black Holes: Evolution, Theory and Thermodynamics Nova Publishers, New York, 2012 (2012), arXiv:1201.4463 [hep-ph].

[25] M. Cavaglia, Int.J.Mod.Phys. **A18**, 1843 (2003), arXiv:hep-ph/0210296 [hep-ph].

[26] P. Kanti, Int.J.Mod.Phys. **A19**, 4899 (2004), arXiv:hep-ph/0402168 [hep-ph].

[27] X. Calmet, L. I. Caramete, and O. Micu, JHEP **1211**, 104 (2012), arXiv:1204.2520 [hep-ph].

[28] N. Arsene, X. Calmet, L. I. Caramete, and O. Micu, (2013), arXiv:1303.4603 [hep-ph].

[29] Y. Luo, S. Cui, X. Ma, J. Zhao, and C. Feng, (2013), arXiv:1309.3973 [astro-ph.HE].

[30] S. Chatrchyan *et al.* (CMS Collaboration), JHEP **1301**, 013 (2013), arXiv:1210.2387 [hep-ex].

[31] G. Aad *et al.* (ATLAS Collaboration), JHEP **1301**, 029 (2013), arXiv:1210.1718 [hep-ex].

[32] J. Abraham *et al.* (Pierre Auger Collaboration), Nucl.Instrum.Meth. **A523**, 50 (2004).

[33] H. Tokuno, Y. Tameda, M. Takeda, K. Kadota, D. Ikeda, *et al.*, Nucl.Instrum.Meth. **A676**, 54 (2012), arXiv:1201.0002 [astro-ph.IM].

[34] 1244641, (2013), arXiv:1307.7071 [astro-ph.IM].

[35] T. K. Gaisser and A. M. Hillas, Proc. 15th Int. Cosmic Ray Conf. (Plovdiv) **8**, 353 (1977).

[36] D. Heck and J. Knapp, Report **FZKA 6097** (1998), Forschungszentrum Karlsruhe; available from http://www-ik.fzk.de/˜heck/publications/ (1989).

[37] D. Heck, J. Knapp, J. Capdevielle, G. Schatz, and T. Thouw, Report **FZKA 6019** (1998), Forschungszentrum Karlsruhe; available from http://www-ik.fzk.de/corsika/physics_description/corsika_phys.html (1998).

[38] H. Yoshino and Y. Nambu, Phys.Rev. **D66**, 065004 (2002), arXiv:gr-qc/0204060 [gr-qc].

[39] D. Allard, N. Busca, G. Decerprit, A. Olinto, and E. Parizot, JCAP **0810**, 033 (2008), arXiv:0805.4779 [astro-ph].

[40] The Pierre Auger Collaboration, P. Abreu, M. Aglietta, E. J. Ahn, I. F. M. Albuquerque, D. Allard, I. Allekotte, J. Allen, P. Allison, J. Alvarez Castillo, and et al., ArXiv e-prints (2011), arXiv:1107.4809 [astro-ph.HE].

[41] J. Abraham, P. Abreu, M. Aglietta, C. Aguirre, D. Allard, I. Allekotte, J. Allen, P. Allison, J. Alvarez-Muñiz, M. Ambrosio, and et al., Physical Review Letters **101**, 061101 (2008), arXiv:0806.4302.

[42] N. N. Kalmykov, S. S. Ostapchenko, and A. I. Pavlov, Nuclear Physics B Proceedings Supplements **52**, 17 (1997).

[43] T. Bergmann, R. Engel, D. Heck, N. Kalmykov, S. Ostapchenko, *et al.*, Astropart.Phys. **26**, 420 (2007), arXiv:astro-ph/0606564 [astro-ph].

[44] N. Kalmykov and S. Ostapchenko, Phys.Atom.Nucl. **56**, 346 (1993).

[45] S. Ostapchenko, Nucl.Phys.Proc.Suppl. **151**, 143 (2006), arXiv:hep-ph/0412332 [hep-ph].

[46] T. Pierog and K. Werner, Phys.Rev.Lett. **101**, 171101 (2008), arXiv:astro-ph/0611311 [astro-ph].

[47] E.-J. Ahn, R. Engel, T. K. Gaisser, P. Lipari, and T. Stanev, Phys.Rev. **D80**, 094003 (2009), arXiv:0906.4113 [hep-ph].